Filomat 34:2 (2020), 303–321
https://doi.org/10.2298/FIL2002303H

Published by Faculty of Sciences and Mathematics,
University of Niš, Serbia
Available at: http://www.pmf.ni.ac.rs/filomat

A Non-Iterative Reconstruction Method for Bioluminescence Tomography

Mourad Hrizi[a]

[a] *Monastir University, Department of Mathematics, Faculty of Sciences Avenue de l'Environnement* 5000, *Monastir, Tunisia*

Abstract. In this paper, we study an inverse source problem of the bioluminescence tomography in three dimensional case. Our aim is to reconstruct a bioluminescent source distribution within a body from the knowledge of the boundary measurements. The inverse source problem is reformulated as a topology optimization one minimizing an energy like type functional. It measures the difference between the solutions of two auxiliary boundary value problems. An asymptotic expansion of the considered functional with respect to a set of ball-shaped anomalies is computed using the topological sensitivity analysis method. The obtained theoretical result leads to build a non-iterative reconstruction algorithm. Finally, some numerical examples in $3D$ are presented in order to show the effectiveness of the devised reconstruction algorithm.

1. Introduction

The inverse problem identifying the source in Partial Differential Equations (PDEs) from overdetermined boundary data have been involved in several areas of science and engineering covering a wide spectrum of applications: Environmental applications [7, 8, 20], Medical applications [1] and Bioluminescence tomography [42].

In this work, we are interested in the inverse problem of the bioluminescence tomography that consists of determining an internal bioluminescent source distribution generated by luciferase inducted by reporter genes [42]. More precisely, we work with the simplest mathematical model for the bioluminescence tomography in three dimensional case which is the diffusion approximation of the radiative transport equation [21]: Then, let Ω be an open bounded domain of $\mathbb{R}^3$ with sufficiently regular boundary $\partial\Omega$. Let $\psi : \Omega \to \mathbb{R}$ denote the photon density. Thus,

$$-\mathrm{div}(\mathcal{D}\nabla\psi) + \mu\psi = f^* \quad \text{in } \Omega. \tag{1}$$

where f^* represents the bioluminescent source function. Moreover, we assume that the absorption coefficient $\mu \geq 0$ as well as the diffusion coefficient $\mathcal{D} \geq \mathcal{D}_0 > 0$ for some positive constant $\mathcal{D}_0$.

The main purpose of this work concerns the problem of recovering the bioluminescent source f^* in the diffusion equation (1) from the Cauchy data $(\partial_\nu\psi_{|\Gamma},\ \psi_{|\Gamma})$ prescribed on the boundary $\Gamma = \partial\Omega$ where $\partial_\nu = \frac{\partial .}{\partial \nu}$ and ν is the outward unit normal to Γ.

2010 *Mathematics Subject Classification*. 35A15, 35B20, 49K40, 65R32.
Keywords. Bioluminescence tomography; Inverse source problem; Topological sensitivity analysis; Kohn-Vogelius formulation; Calculus of variations.
Received: 23 February 2019; Revised: 22 January 2020; Accepted: 02 February 2020
Communicated by Miodrag Spalević
Email address: mourad-hrizi@hotmail.fr (Mourad Hrizi)

The major difficulty of this inverse source problem from boundary data concerns the non-uniqueness of general sources term, see [21, Corollary 2.4] for example. Theoretically, the bioluminescent source uniqueness shows that a priori information has a quite effect on source detection. Here, to cope with these difficulties the source term f^* is modeled as a linear combination of a finite number of solid ball sources, namely,

$$f^*(x) = \sum_{i=1}^{m} \gamma_i \chi(\omega_i^*) \text{ with } \omega_i^* \cap \omega_j^* = \emptyset \text{ for all } i \neq j \text{ and } i, j \in \{1, ..., m\}, \tag{2}$$

where $\omega_i^* \subset \Omega$ is a solid ball of center $s_i^* \in \Omega$ and radii r_i^*, that is,

$$\omega_i^* = \{x \in \mathbb{R}^3 : \ |x - s_i^*| < r_i^*\},$$

with $\chi(\omega_i^*)$ is the characteristic function of the set ω_i^*, m is a given non-negative integer, the intensity γ_i is non-null scalar. See the sketch in Figure 1.

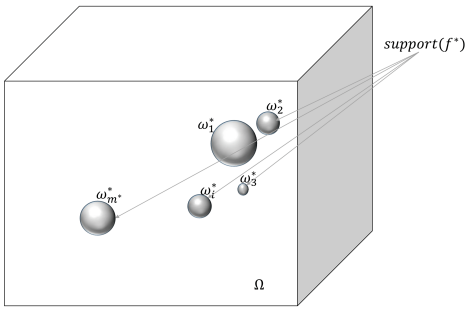

Figure 1: The inverse source problem.

Practically, we know that the source intensity is closely related to the strength of the molecular/cellular activity, such as gene expression. Thus, it is often reasonable to take the intensity or its parametric form as known to find the unique solution. Hence, in this article, we assume that the source intensity γ_i is known and we reconstruct the geometrical support of the sources $\omega^* = \cup_{i=1}^m \omega_i^*$ with the help of the Cauchy data $(\partial_\nu \psi_{|\Gamma}, \ \psi_{|\Gamma})$. In addition, for the sake of simplicity, we assume that $\gamma_1 = ... = \gamma_m = \gamma$.

Then our inverse source problem is formulated as follows: given $\gamma \in \mathbb{R}^*$, $\mathcal{D} > 0$, $\mu \geq 0$, and $(\varphi, \phi) \in H^{-1/2}(\Gamma) \times H^{1/2}(\Gamma)$, reconstruct the source term $f^* = \sum_{i=1}^m \gamma \chi(\omega_i^*)$ (i.e $\omega^* = \cup_{i=1}^m \omega_i^*$) such that the solution of the following boundary value problem

$$\begin{aligned} -\text{div}(\mathcal{D}\nabla\psi) + \mu\psi &= f^* \quad \text{in } \Omega, \\ \mathcal{D}\partial_\nu \psi &= \varphi \quad \text{on } \Gamma, \end{aligned} \tag{3}$$

satisfies

$$\psi = \phi \quad \text{on } \Gamma. \tag{4}$$

In the literature, there have been many authors who were interested in similar works. In the particular case $\mu = 0$, in [9, 23, 27, 28, 33] the authors applied some iterative algorithm to reconstruct the shape of a source. In the case $\mu \neq 0$ (with $\mu = -k^2$ and $\mathcal{D} = 1$) EL Badia and Nara in [18] proposed a direct method the so-called algebraic method, requires algebraic relationships between source parameters and observable data. For the diffusion equation in [11, 13, 21, 22] the authors used a regularization procedure performed to determine the source function $f^* = \gamma\chi(\omega^*)$ (i.e $\omega_1^* = ... = \omega_m^* = \omega^*$) such that γ is unknown function and ω^* is a given permissible region about the source function. While Kreutzmann and Rieder [32] reconstructed the

source f^*, using a method based on the minimization of the Mumford-Shah like functional which penalizes the perimeter of the domains ω_i^*, $i = 1, ..., m$. More recently, in the context of source-term problem of the Poisson equation Canelas *et al* [12] proposed a reconstruction approach based on the minimization of the $L^2(\Omega)$-norm of the error function by using the topological derivative method. Moreover, there have been closer works to our problem was presented in [2, 14–17, 39, 40].

In this paper, we follow the approach introduced in [26] (see also [25]) and we propose a non-iterative algorithm for the reconstruction of the source term f^* from a single Cauchy data, but without using the Newtonian potential to complement the unavailable information about the hidden boundary as presented in [12]. The proposed approach is based on the advantage of the Kohn-Vogelius formulation [31] and the topological sensitivity analysis method [3, 19]. The Kohn-Vogelius formulation is a self regularization technique and rephrases the inverse source problem as a topology optimization problem, where the support of the bioluminescent source is the unknown variable. The main advantage of the proposed approach is that, it provides fast and accurate results for detection (location and shape).

The main contribution of this work concerns the theoretical and numerical aspects. In the theoretical part, we study the diffusion equation in the three dimensional case. We derive a topological sensitivity of an energy like functional with respect to a set of ball-shaped sources. In the numerical part, from the obtained theoretical results, we present a non-iterative reconstruction algorithm to recover the location, shape and the size of a hidden source within a body in $3D$ domain.

The outline of the paper is as follows. In Section 2, we prove that the considered inverse problem does not have a unique solution when we want to determine both, the topology of ω^* and the intensity γ. Then, Section 3 is devoted to solve the inverse problem. In Section 4, we derive a topological asymptotic expansion of an energy like functional with respect to a finite number of perturbed source. Based of this asymptotic expansion, we propose in Section 5 a fast and accurate reconstruction algorithm.

2. Non-uniqueness result

As is pointed out in the introduction, without a priori information on the source, the uniqueness is not guaranteed for general sources. We consider in this section the sources f^* of the form

$$f^* = \gamma\chi(\omega) \text{ with } \omega = \{x \in \mathbb{R}^3 : \ 0 \leq r_0 < |x - s^*| < r_1\}, \tag{5}$$

where $s^* \in \Omega$ and $\omega \subset \Omega$ is hollow ball if $r_0 > 0$ and a solid ball if $r_0 = 0$.

The purpose of this section is to prove that the inverse problem (3)-(4) cannot be solved uniquely when both, the topology of ω^* and the intensity γ, are unknown simultaneously.

Before establishing non-uniqueness result, for sources term of the form (5), we need the following lemma for the diffusion equation given in [42, Lemma D.2]:

Lemma 2.1. *For any constant $\mathcal{D} > 0$, $\mu \geq 0$ and any solution ψ_0 of*

$$-div(\mathcal{D}\nabla\psi_0) + \mu\psi_0 = 0 \text{ in } \ \mathrm{B}_R(x_0),$$

we have

$$\int_{r_0<|x-x_0|<r_1} \psi_0 dx = \left(\int_{r_0}^{r_1} V_d r^{d-1}\xi(r)\, dr\right)\psi_0(x_0),$$

where $\mathrm{B}_R(x_0)$ is the sphere of center x_0 and radius R, $0 \leq r_0 < r_1 < R$, V_d is the surface area of the unit sphere in $\mathbb{R}^d$, and $\xi(r)$ is the unique positive radial solution of

$$-\mathcal{D}\Delta\xi + \mu\xi = -\mathcal{D}\left(\xi'' + \frac{d-1}{r}\xi'\right) + \mu\xi = 0$$

with $\xi(0) = 1$ and $\xi'(0) = 0$. Moreover, we have, for $\mu = 0$,

$$\xi(r) = 1,$$

and for $\mu > 0$,

$$\xi(r) = \begin{cases} \mathbf{J}_0(\sqrt{\frac{\mu}{\mathcal{D}}}r), & \text{if } d = 2 \\ \dfrac{\sinh(\sqrt{\frac{\mu}{\mathcal{D}}}r)}{\sqrt{\frac{\mu}{\mathcal{D}}}r}, & \text{if } d = 3, \end{cases}$$

where $\mathbf{J}_0$ *is a Bessel function of the first kind.*

Now, we prove that both the intensity γ and the domain ω cannot uniquely be reconstructed from the Cauchy data. To do that one has to establish two different sources $f_i^* = \gamma_i \chi(\omega_i)$and two functions ψ_i such that

$$-\mathrm{div}(\mathcal{D}\nabla\psi_i) + \mu\psi_i = f_i^* \quad \text{in } \Omega,\ \psi_1 = \psi_2,\ \partial_\nu\psi_1 = \partial_\nu\psi_2 \text{ on } \Gamma.$$

Let $f_i^* = \gamma_i\chi(\omega_i)$, $i = 1, 2$, where ω_i are two hollow or solid balls with same center x_0 and different radii r_0^i, r_1^i, such that

$$\gamma_1 \int_{r_0^1}^{r_1^1} r^2 \frac{\sinh(\sqrt{\frac{\mu}{\mathcal{D}}}r)}{\sqrt{\frac{\mu}{\mathcal{D}}}r}\,\mathrm{dr} = \gamma_2 \int_{r_0^2}^{r_1^2} r^2 \frac{\sinh(\sqrt{\frac{\mu}{\mathcal{D}}}r)}{\sqrt{\frac{\mu}{\mathcal{D}}}r}\,\mathrm{dr}. \tag{6}$$

Define the function w by

$$\begin{aligned} -\mathrm{div}(\mathcal{D}\nabla w) + \mu w &= f_2^* - f_1^* \quad \text{in } \Omega, \\ w &= 0 \quad \text{on } \Gamma, \end{aligned} \tag{7}$$

and let ϑ be an arbitrary function in the space of the homogeneous diffusion equation $\mathcal{V}_\mu$ defined by

$$\mathcal{V}_\mu = \{\vartheta \in \mathrm{H}^1(\Omega) :\ -\mathrm{div}(\mathcal{D}\nabla\vartheta) + \mu\vartheta = 0\}.$$

By multiplying the first equation of (7) by ϑ and by integrating parts, we have

$$-\int_\Gamma \partial_\nu w\ \vartheta \mathrm{d}s + \int_\Gamma \partial_\nu\vartheta\ w\mathrm{d}s = \gamma_2 \int_{\omega_2} \vartheta \mathrm{d}x - \gamma_1 \int_{\omega_1} \vartheta \mathrm{d}x. \tag{8}$$

Thus, from lemma 2.1, one has

$$\int_{\omega_i} \vartheta \mathrm{d}x = 4\pi\vartheta(x_0) \int_{r_0^i}^{r_1^i} r^2 \frac{\sinh(\sqrt{\frac{\mu}{\mathcal{D}}}r)}{\sqrt{\frac{\mu}{\mathcal{D}}}r}\,\mathrm{dr}, \quad i = 1, 2.$$

Then, we deduce that

$$-\int_\Gamma \partial_\nu w\ \vartheta \mathrm{d}s + \int_\Gamma \partial_\nu\vartheta\ w\mathrm{d}s = \gamma_2 4\pi\vartheta(x_0) \int_{r_0^2}^{r_1^2} r^2 \frac{\sinh(\sqrt{\frac{\mu}{\mathcal{D}}}r)}{\sqrt{\frac{\mu}{\mathcal{D}}}r}\,\mathrm{dr} - \gamma_1 4\pi\vartheta(x_0) \int_{r_0^1}^{r_1^1} r^2 \frac{\sinh(\sqrt{\frac{\mu}{\mathcal{D}}}r)}{\sqrt{\frac{\mu}{\mathcal{D}}}r}\,\mathrm{dr}.$$

Consequently, from (6) and (7), we obtain

$$\int_\Gamma \partial_\nu w\ \vartheta \mathrm{d}s = \int_\Gamma \partial_\nu\vartheta\ w\mathrm{d}s = 0.$$

Moreover, using that $H^{1/2}(\Gamma)$ is dense in $L^2(\Gamma)$ [10], we get:

$$\partial_\nu w = 0 \ \text{ on } \Gamma.$$

Therefore, the desired result is obtained by choosing the functions ψ_1 and $\psi_2 = \psi_1 + w$.

Remark 2.2. *A similar result is obtained for the Helmholtz equation was presented in [18].*

Next, we present the proposed approach to solve the inverse source problem (3)-(4).

3. Problem reformulation

Since the considered inverse problem is written in the form of an ill-posed boundary value problem, the idea is to rewrite it as a topology optimization problem. In particular, an energy like functional is minimized with respect to a set of ball-shaped anomalies by using the concept of topological sensitivity. More precisely, Subsection 3.1, is devoted to minimize the misfit between the solutions of two forward problems that contain information on the boundary measurements. In other words, we minimize a Kohn-Vogelius type functional obtained from the Kohn-Vogelius formulation. While in Subsection 3.2, we introduce the topological sensitivity analysis method to minimize this functional.

We define the following class of admissible sources:

$$\mathcal{U}_{ad}(\Omega) := \{h \in L^\infty(\Omega) : \ h = \gamma\chi(\omega), \ \omega \subset \Omega \text{ is a Lebesgue measurable set}\}.$$

Here, $\chi(\omega)$ denotes the indicator function of the set ω and $\gamma \in \mathbb{R}^*$ is given. Moreover, we assume that the sets ω in $\mathcal{U}_{ad}(\omega)$ are of the form:

$$\omega = \bigcup_{i=1}^{m} \omega_i \text{ with } \overline{\omega_i} \cap \overline{\omega_j} = \emptyset \text{ for } i \neq j \text{ and } i, j \in \{1, ..., m\},$$

where each $\omega_i \subset \Omega$ is a solid ball of center $s_i \in \Omega$ and radii r_i, that is,

$$\omega_i = \{x \in \mathbb{R}^3 : \ |x - s_i| < r_i\}.$$

3.1. The Kohn-Vogelius formulation

The Kohn-Vogelius formulation is a self regularization technique and rephrase the considered inverse source problem into a topology optimization one. It leads to define for any given source $f \in \mathcal{U}_{ad}(\Omega)$ two auxiliary problems. The first one is associated to the Neumann datum φ, which will be named as the "*Neumann problem*":

$$\begin{aligned} -\text{div}(\mathcal{D}\nabla\psi_N[f]) + \mu\psi_N[f] &= f \quad \text{in } \Omega, \\ \mathcal{D}\partial_\nu\psi_N[f] &= \varphi \quad \text{on } \Gamma. \end{aligned} \tag{9}$$

The second one is associated to the Dirichlet (measured) datum ϕ :

$$\begin{aligned} -\text{div}(\mathcal{D}\nabla\psi_D[f]) + \mu\psi_D[f] &= f \quad \text{in } \Omega, \\ \psi_D[f] &= \phi \quad \text{on } \Gamma. \end{aligned} \tag{10}$$

The existence and the uniqueness of $\psi_N[f]$ and $\psi_D[f]$ is guaranteed by Lax-Milgram Lemma [10]. Notice that in the particular case $\mu = 0$, the problem (9) has a unique solution up to an additive constant. To ensure uniqueness, the boundary force φ and the source f should satisfy the compatibility condition:

$$\int_\Omega f \, \mathrm{d}x + \int_\Gamma \varphi \, \mathrm{d}s = 0.$$

One can remark that if $\omega = \cup_{i=1}^m \omega_i$ coincides with the actual support sources $\omega^* = \cup_{i=1}^m \omega_i^*$ (i.e $f^* = f$) then $\psi_N[f] = \psi_D[f]$ in Ω. According to this observation, we propose a reconstruction process based on the minimization of the so-called Kohn-Vogelius functional :

$$\mathcal{J}(f) = \int_\Omega \mathcal{D}\Big|\nabla\Big(\psi_N[f] - \psi_D[f]\Big)\Big|^2 \, \mathrm{d}x.$$

Thus, the inverse source problem can be formulated as an optimization problem as follows :

$$\text{Find the source term } f^* = \sum_{i=1}^{m} \gamma\chi(\omega_i^*) \text{ such that } \mathcal{J}(f^*) = \min_{f\in\mathcal{U}_{ad}(\Omega)} \mathcal{J}(f). \tag{11}$$

Remark 3.1. *It is not difficult to verify that for any $f, g \in L^\infty(\Omega)$,*

$$\mathcal{J}(tf + (1-t)g) \leq t\mathcal{J}(f) + (1-t)\mathcal{J}(g) \text{ for all } t \in (0,1).$$

Hence, the functional $\mathcal{J}$ is convex.

The theoretical aspect of the inverse source problem for the diffusion equation (3)-(4) has been the subject of various researcher's works. Particularly, in [42] Wang *et al.* discussed the uniqueness solution of the inverse source problem (3)-(4) in the two and three dimensional cases. They established the uniqueness in determining the bioluminescent source f^* from a measurement on a part P_0 of the exterior boundary Γ. Thus, we have the following identifiability theorem from [42, Theorem IV.3]:

Theorem 3.2. *Let*

$$f_1(y) = \sum_{i=1}^{n} \gamma_i\chi(\mathcal{B}_{r_0^i,r_1^i}(x_i)) \text{ and } f_2(y) = \sum_{i=1}^{M} \Lambda_i\chi(\mathcal{B}_{R_0^i,R_1^i}(X_i))$$

be two solutions to the problem (3)-(4), then $n = M$ and there exist a permutation τ of $[1,n]$ and a map $C : [1,n] \to [1,T]$ such that $x_i = X_{\tau(i)}$ and

$$\gamma_i \int_{r_0^i}^{r_1^i} r^{d-1}\xi_{C(i)}(r)dr = \Lambda_{\tau(i)} \int_{R_0^{\tau(i)}}^{R_1^{\tau(i)}} r^{d-1}\xi_{C(i)}(r)dr, \text{ for } i = 1,...,T,$$

where $\mathcal{B}_{r,R}(z) = \{x \in \mathbb{R}^d : r < |x-z| < R\}$ with $d \in \{2,3\}$, $0 \leq r < R < \infty$ and ξ_i is the unique solution of

$$-\mathcal{D}_i\left(\xi_i'' + \frac{d-1}{r}\xi_i'\right) + \mu_i\xi_i = 0,$$
$$\xi_i(0) = 1, \quad \xi_i'(0) = 0.$$

The following corollary follows from the identifiability Theorem 3.2. It gives the uniqueness solution of the considered inverse problem.

Corollary 3.3. *The source term $f^* = \sum_{i=1}^m \gamma\chi(\omega_i^*)$ (see (2)) and the function ψ that satisfy (3) and (4) are uniquely defined by the nontrivial Cauchy data (φ, ϕ).*

Proof. The proof of this corollary is a direct consequence of Theorem 3.2 and Lemma 2.1. □

Thanks to Corollary 3.3, we obtain the following uniqueness result of the minimization problem (11):

Lemma 3.4. *Let $(\varphi, \phi) \in H^{-1/2}(\Gamma) \times H^{1/2}(\Gamma)$ be given nontrivial Cauchy data. If $f^* = \sum_{i=1}^m \gamma\chi(\omega_i^*) \in \mathcal{U}_{ad}(\Omega)$ is the solution of the inverse problem with respect to the data (φ, ϕ) then f^* is the unique equilibrium function of the Kohn-Vogelius cost functional $\mathcal{J}$:*

$$\mathcal{J}(f^*) \leq \mathcal{J}(f) \text{ for all } f \in \mathcal{U}_{ad}(\Omega).$$

Proof. If $f^* = \sum_{i=1}^m \gamma\chi(\omega_i^*) \in \mathcal{U}_{ad}(\Omega)$ is the solution of the overdetermined problem (3)-(4), then $\phi = \psi_N[f^*] +$ *constant* which implies $\nabla\psi_N[f^*] = \nabla\psi_D[f^*]$. Consequently, f^* will be the minimum of the functional $\mathcal{J}$ with $\mathcal{J}(f^*) = 0$. Let $f = \sum_{i=1}^m \gamma\chi(\omega_i) \in \mathcal{U}_{ad}(\Omega)$ be another minimizer of $\mathcal{J}$. Then $\psi_N[f]$ verifies problem (3) with $\psi_N[f] = \phi$ on Σ. From the Corollary 3.3, we get $\omega_i = \omega_i^*$ for $i = 1,...,m$(i.e $f = f^*$). □

Now, to solve the optimization problem (11), we apply a method based on the concept of the topological sensitivity. This concept was originally introduced by Sokolowski and Zochowski [38]. Since then, this concept has been successfully applied to many relevant scientific and engineering problems such as geometry inverse problems [5, 25, 30, 37], topology optimization [3, 6, 34, 35], structural mechanics [19, 41], image processing [24, 29], and damage evolution modeling [4], and many other applications.

3.2. Topological sensitivity analysis

The topological sensitivity analysis consists to study the variations of a given shape functional with respect to the insertion of a small topological perturbation, such as cavities, inclusions, source-terms or even cracks. For more details about this approach we refer the reader to the book by Novotny and Sokolowski [36] and references therein.

To present the main idea of this method, let us consider a geometry perturbation of ω_i, $1 \leq i \leq m$, confined in a small set $\omega_{z_i,\varepsilon} = z_i + \varepsilon O_i$ where $\varepsilon > 0$, $z_i \in \Omega$ and $O_i \subset \mathbb{R}^3$ is a given fixed and bounded domain containing the origin. We consider the particular case $\omega_{z_i,\varepsilon} = \mathcal{B}_\varepsilon(z_i)$, where $\mathcal{B}_\varepsilon(z_i)$ is a small ball of radius ε and center $z_i \in \Omega$ for $i = 1, ..., m$. Moreover, we assume that $\overline{\mathcal{B}_\varepsilon(z_i)} \cap \Gamma = \emptyset$ and $\overline{\mathcal{B}_\varepsilon(z_i)} \cap \overline{\mathcal{B}_\varepsilon(z_j)} = \emptyset$ for each $i \neq j$ and $i, j \in \{1, ..., m\}$.

To this end, for a given source term f in the diffusion equation (1), let $\delta f_{z,\varepsilon}$ be a finite topological perturbation of f on the form

$$\delta f_{z,\varepsilon}(x) = \sum_{i=1}^{m} \gamma \chi(\mathcal{B}_\varepsilon(z_i)), \tag{12}$$

where $z = (z_1, ..., z_m) \in \Omega \times ... \times \Omega$. Then the Kohn-Vogelius shape functional $\mathcal{J}$ associated with the topological perturbation $\delta f_{z,\varepsilon}$ is written as

$$\mathcal{J}(f + \delta f_{z,\varepsilon}) = \int_\Omega \mathcal{D} \Big| \nabla \Big(\psi_N[f + \delta f_{z,\varepsilon}] - \psi_D[f + \delta f_{z,\varepsilon}] \Big) \Big|^2 \, \mathrm{d}x,$$

with $\psi_N[f + \delta f_{z,\varepsilon}]$ be the solution of the perturbed Neumann boundary value problem

$$\begin{aligned} -\mathrm{div}(\mathcal{D} \nabla \psi_N[f + \delta f_{z,\varepsilon}]) + \mu \psi_N[f + \delta f_{z,\varepsilon}] &= f + \delta f_{z,\varepsilon} \quad \text{in } \Omega, \\ \mathcal{D} \partial_\nu \psi_N[f + \delta f_{z,\varepsilon}] &= \varphi \quad \text{on } \Gamma \end{aligned} \tag{13}$$

and $\psi_D[f + \delta f_{z,\varepsilon}]$ be the solution of the perturbed Dirichlet boundary value problem

$$\begin{aligned} -\mathrm{div}(\mathcal{D} \nabla \psi_D[f + \delta f_{z,\varepsilon}]) + \mu \psi_D[f + \delta f_{z,\varepsilon}] &= f + \delta f_{z,\varepsilon} \quad \text{in } \Omega, \\ \psi_D[f + \delta f_{z,\varepsilon}] &= \phi \quad \text{on } \Gamma. \end{aligned} \tag{14}$$

From these elements, the topological sensitivity analysis leads to an asymptotic expansion of the shape functional $\mathcal{J}$ of the form,

$$\mathcal{J}(f + \delta f_{z,\varepsilon}) = \mathcal{J}(f) + \zeta(\varepsilon) \delta \mathcal{J}(z) + o(\zeta(\varepsilon)), \text{ for all } z_i \in \Omega, \tag{15}$$

where

• $\varepsilon \mapsto \zeta(\varepsilon)$ is a scalar positive function such that $\zeta(\varepsilon) \to 0$, when $\varepsilon \to 0$.

• The function $z \mapsto \delta \mathcal{J}(z)$ is independent of ε and it is called the "topological sensitivity" or "topological gradient" of $\mathcal{J}$ at z. Therefore, this gradient can be seen as a first order correction of $\mathcal{J}(f)$ to approximate $\mathcal{J}(f + \delta f_{z,\varepsilon})$. In particular, after rearranging (15) we obtain

$$\frac{\mathcal{J}(f + \delta f_{z,\varepsilon}) - \mathcal{J}(f)}{\zeta(\varepsilon)} = \delta \mathcal{J}(z) + \frac{o(\zeta(\varepsilon))}{\zeta(\varepsilon)}.$$

The limit passage $\varepsilon \to 0$ in the above expression leads to the definition for the topological gradient

$$\delta \mathcal{J}(z) := \lim_{\varepsilon \to 0} \frac{\mathcal{J}(f + \delta f_{z,\varepsilon}) - \mathcal{J}(f)}{\zeta(\varepsilon)}.$$

Hence, if we want to minimize the functional $\mathcal{J}$, the best location of the source function $\delta f_{z,\varepsilon}$ in Ω is where the so-called topological gradient $\delta \mathcal{J}$ is most negative. In fact if $\delta \mathcal{J}(z) < 0$, we have $\mathcal{J}(f + \delta f_{z,\varepsilon}) < \mathcal{J}(f)$ for small $\varepsilon > 0$. Particularly, if $f = 0$ the solution of the minimization problem;

$$\min_{\delta f_{z,\varepsilon} \in \mathcal{U}_{ad}(\Omega)} \mathcal{J}(\delta f_{z,\varepsilon})$$

is given by $\delta f^*_{z^*,\varepsilon} = \sum_{i=1}^{m} \gamma\chi(\mathcal{B}_\varepsilon(z_i^*))$, such that $\delta\mathcal{J}(z^*) < 0$ and $\delta\mathcal{J}(z^*) < \delta\mathcal{J}(z)$, for all $z \in \Omega^m$.

Next, we calculate the exact expression of the function ζ and the topological gradient $\delta\mathcal{J}$.

4. Asymptotic expansion

In this section, we derive a topological sensitivity analysis for the diffusion equation with respect to a small topological perturbation of the source term. More precisely, for a given source term f in the diffusion equation (1), we study the variation of the Kohn-Vogelius functional $\mathcal{J}$ with respect to a finite topological perturbation $\delta f_{z,\varepsilon}$ defined in (12) of f on the form (15).

Let us introduce $\theta_N[f]$ and $\theta_D[f]$ are solutions to the following adjoint problems:

$$\begin{cases} \text{Find } \theta_N[f] \in H^1(\Omega), \text{ such that} \\ \mathcal{A}(w, \theta_N[f]) = -2\displaystyle\int_\Omega \mathcal{D}\nabla(\psi_N[f] - \psi_D[f]).\nabla w \mathrm{d}x \text{ for all } w \in H^1(\Omega), \end{cases} \tag{16}$$

$$\begin{cases} \text{Find } \theta_D[f] \in H^1_0(\Omega), \text{ such that} \\ \mathcal{A}(w, \theta_D[f]) = -2\displaystyle\int_\Omega \mathcal{D}\nabla(\psi_D[f] - \psi_N[f]).\nabla w \mathrm{d}x \text{ for all } w \in H^1_0(\Omega), \end{cases} \tag{17}$$

with

$$\mathcal{A}(u, v) = \int_\Omega \mathcal{D}\nabla u.\nabla v \, \mathrm{d}x + \mu \int_\Omega u\, v \, \mathrm{d}x \text{ for all } u, v \in \mathrm{H}^1(\Omega).$$

The following theorem gives us the topological asymptotic expansion of the Kohn-Vogelius functional $\mathcal{J}$:

Theorem 4.1. *Let $\delta f_{z,\varepsilon}$ be a small topological perturbation defined in (12) of a given source term f, then the Kohn-Vogelius functional $\mathcal{J}$ admits the following topological asymptotic expansion:*

$$\mathcal{J}(f + \delta f_{z,\varepsilon}) = \mathcal{J}(f) + \varepsilon^3 \sum_{i=1}^{m} \delta\mathcal{J}(z_i) + o(\varepsilon^3), \tag{18}$$

with $\delta\mathcal{J}$ is the topological gradient given by

$$\delta\mathcal{J}(x) = \frac{4\pi}{3}\gamma(\theta_N(x) + \theta_D(x)), \text{ for all } x \in \Omega.$$

To prove Theorem 4.1, we need to establish the following preliminary lemma.

Lemma 4.2. *Let $\psi_N[f + \delta f_{z,\varepsilon}]$ and $\psi_D[f + \delta f_{z,\varepsilon}]$ be the solutions to the perturbed value problems (13) and (14), respectively. Then there exists a constant $c > 0$, independent of ε, such that the inequalities*

$$\left\|\psi_N[f + \delta f_{z,\varepsilon}] - \psi_N[f]\right\|_{H^1(\Omega)} \leq c\varepsilon^{5/2}, \tag{19}$$

$$\left\|\psi_D[f + \delta f_{z,\varepsilon}] - \psi_D[f]\right\|_{H^1(\Omega)} \leq c\varepsilon^{5/2}. \tag{20}$$

are satisfied for any small parameter $\varepsilon > 0$.

Proof. Here, we will prove only the estimate (19) and the other estimate is treated analogous.
Posing $u_N[f] = \psi_N[f + \delta f_{z,\varepsilon}] - \psi_N[f]$. One can easily remark that $u_N[f]$ is solution to the system

$$\begin{aligned} -\mathrm{div}(\mathcal{D}\nabla u_N[f]) + \mu\, u_N[f] &= \delta f_{z,\varepsilon} \quad \text{in } \Omega, \\ \mathcal{D}\partial_\nu u_N[f] &= 0 \quad \text{on } \Gamma. \end{aligned} \tag{21}$$

The variational formulation of (21) is: find $u_N[f] \in H^1(\Omega)$ such that

$$\begin{aligned}\int_\Omega \mathcal{D}\nabla u_N[f].\nabla\xi \mathrm{d}x + \mu \int_\Omega u_N[f]\xi \mathrm{d}x \\ = \int_\Omega \delta f_{z,\varepsilon}\xi \mathrm{d}x, \text{ for all } \xi \in H^1(\Omega).\end{aligned} \tag{22}$$

By taking $\xi = u_N[f]$ in (22) as a test function, we have

$$\int_\Omega \mathcal{D}|\nabla u_N[f]|^2 \mathrm{d}x + \int_\Omega \mu |u_N[f]|^2 \mathrm{d}x = \int_\Omega \delta f_{z,\varepsilon} u_N[f] \mathrm{d}x. \tag{23}$$

Then, there exists a constant $c > 0$, independent of ε, such that

$$\|u_N[f]\|^2_{H^1(\Omega)} \leq c \int_\Omega \left|\delta f_{z,\varepsilon} u_N[f]\right| \mathrm{d}x.$$

Using Hölder inequality ($p = 6/5$ and $q = 6$) and the fact that $H^1(\Omega) \hookrightarrow L^6(\Omega)$ (see for example [10]), it follows

$$\int_\Omega \left|\delta f_{z,\varepsilon} u_N[f]\right| \mathrm{d}x \leq c\|\delta f_{z,\varepsilon}\|_{L^{6/5}(\Omega)}\|u_N[f]\|_{L^6(\Omega)} \leq c\|\delta f_{z,\varepsilon}\|_{L^{6/5}(\Omega)}\|u_N[f]\|_{H^1(\Omega)}.$$

From the definition of $\delta f_{z,\varepsilon}$ (see (12)) and the fact that $|\mathcal{B}_\varepsilon(z_i)| \sim \frac{4\pi}{3}\varepsilon^3$, we obtain

$$\begin{aligned}\|u_N[f]\|^2_{H^1(\Omega)} &\leq c \sum_{i=1}^m |\mathcal{B}_\varepsilon(z_i)|^{5/6}\|u_N[f]\|_{H^1(\Omega)} \\ &\leq c\varepsilon^{5/2}\|u_N[f]\|_{H^1(\Omega)}.\end{aligned}$$

Hence,

$$\|\psi_N[f + \delta f_{z,\varepsilon}] - \psi_N[f]\|_{H^1(\Omega)} = \|u_N[f]\|_{H^1(\Omega)} \leq c\varepsilon^{5/2}.$$

□

Now, we are ready to prove the Theorem 4.1.

Proof of Theorem 4.1.. The Kohn-Vogelius functional $\mathcal{J}$ can be decomposed as

$$\mathcal{J}(f + \delta f_{z,\varepsilon}) = \mathcal{J}_{NN}(f + \delta f_{z,\varepsilon}) + \mathcal{J}_{DD}(f + \delta f_{z,\varepsilon}) - 2\,\mathcal{J}_{DN}(f + \delta f_{z,\varepsilon}),$$

where

$$\begin{aligned}\mathcal{J}_{NN}(f + \delta f_{z,\varepsilon}) &= \int_\Omega \mathcal{D}|\nabla\psi_N[f + \delta f_{z,\varepsilon}]|^2 \,\mathrm{d}x, \\ \mathcal{J}_{DD}(f + \delta f_{z,\varepsilon}) &= \int_\Omega \mathcal{D}|\nabla\psi_D[f + \delta f_{z,\varepsilon}]|^2 \,\mathrm{d}x, \\ \mathcal{J}_{DN}(f + \delta f_{z,\varepsilon}) &= \int_\Omega \mathcal{D}\nabla\psi_D[f + \delta f_{z,\varepsilon}].\nabla\psi_N[f + \delta f_{z,\varepsilon}] \,\mathrm{d}x.\end{aligned}$$

Next, we calculate the variation of each functional $\mathcal{J}_{NN}$, $\mathcal{J}_{DD}$ and $\mathcal{J}_{DN}$ separately.
• ***Variation of*** $\mathcal{J}_{NN}$: the variation of $\mathcal{J}_{NN}$ reads

$$\begin{aligned}\mathcal{J}_{NN}(f + \delta f_{z,\varepsilon}) - \mathcal{J}_{NN}(f) &= \int_\Omega \mathcal{D}|\nabla\psi_N[f + \delta f_{z,\varepsilon}]|^2 \,\mathrm{d}x - \int_\Omega \mathcal{D}|\nabla\psi_N[f]|^2 \,\mathrm{d}x, \\ = 2\int_\Omega \mathcal{D}\nabla\psi_N[f].\nabla(\psi_N[f + \delta f_{z,\varepsilon}] - \psi_N[f]) \,\mathrm{d}x &+ \int_\Omega \mathcal{D}|\nabla(\psi_N[f + \delta f_{z,\varepsilon}] - \psi_N[f])|^2 \,\mathrm{d}x.\end{aligned} \tag{24}$$

Let $\vartheta_N[f] \in H^1(\Omega)$ be the solution of the following auxiliary variational problem:

$$\int_\Omega \mathcal{D}\nabla w.\nabla \vartheta_N[f]\,\mathrm{d}x + \mu \int_\Omega w\ \vartheta_N[f]\,\mathrm{d}x = 2\int_\Omega \mathcal{D}\nabla\psi_N[f].\nabla w\,\mathrm{d}x,\ \text{for all } w \in H^1(\Omega). \tag{25}$$

By taking $w = \psi_N[f + \delta f_{z,\varepsilon}] - \psi_N[f]$ in (25) as a test function, we obtain

$$\begin{aligned}&\int_\Omega \mathcal{D}\nabla(\psi_N[f + \delta f_{z,\varepsilon}] - \psi_N[f]).\nabla\vartheta_N[f]\,\mathrm{d}x + \mu\int_\Omega(\psi_N[f + \delta f_{z,\varepsilon}] - \psi_N[f])\vartheta_N[f]\,\mathrm{d}x\\ &= 2\int_\Omega \mathcal{D}\nabla\psi_N[f].\nabla(\psi_N[f + \delta f_{z,\varepsilon}] - \psi_N[f])\,\mathrm{d}x.\end{aligned} \tag{26}$$

Inserting (26) into (24), we deduce

$$\begin{aligned}\mathcal{J}_{NN}(f + \delta f_{z,\varepsilon}) - \mathcal{J}_{NN}(f) &= \int_\Omega \mathcal{D}\nabla(\psi_N[f + \delta f_{z,\varepsilon}] - \psi_N[f]).\nabla\vartheta_N[f]\,\mathrm{d}x\\ &+ \int_\Omega \mu(\psi_N[f + \delta f_{z,\varepsilon}] - \psi_N[f])\vartheta_N[f]\,\mathrm{d}x + \int_\Omega \mathcal{D}|\nabla(\psi_N[f + \delta f_{z,\varepsilon}] - \psi_N[f])|^2\,\mathrm{d}x.\end{aligned} \tag{27}$$

Choosing $\xi = \vartheta_N[f]$ in (22) as a test function, we get

$$\begin{aligned}\int_\Omega \mathcal{D}\nabla(\psi_N[f + \delta f_{z,\varepsilon}] - \psi_N[f]).\nabla\vartheta_N[f]\mathrm{d}x + \int_\Omega \mu(\psi_N[f + \delta f_{z,\varepsilon}] - \psi_N[f])\vartheta_N[f]\mathrm{d}x&\\ = \int_\Omega \delta f_{z,\varepsilon}\vartheta_N[f]\mathrm{d}x.&\end{aligned}$$

Consequently,

$$\mathcal{J}_{NN}(f + \delta f_{z,\varepsilon}) - \mathcal{J}_{NN}(f) = \int_\Omega \delta f_{z,\varepsilon}\vartheta_N[f]\,\mathrm{d}x + \int_\Omega \mathcal{D}|\nabla(\psi_N[f + \delta f_{z,\varepsilon}] - \psi_N[f])|^2\,\mathrm{d}x.$$

Thanks to Lemma 4.2 and using definition of $\delta f_{z,\varepsilon}$ (see (12)), we obtain

$$\begin{aligned}\mathcal{J}_{NN}(f + \delta f_{z,\varepsilon}) - \mathcal{J}_{NN}(f) &= \int_\Omega \delta f_{z,\varepsilon}\vartheta_N[f]\,\mathrm{d}x + o(\varepsilon^3)\\ &= \sum_{i=1}^m \gamma|\mathcal{B}_\varepsilon(z_i)|\vartheta_N[f](z_i) + \sum_{i=1}^m \int_{\mathcal{B}_\varepsilon(z_i)} \gamma\{\vartheta_N[f] - \vartheta_N[f](z_i)\}\,\mathrm{d}x + o(\varepsilon^3).\end{aligned}$$

Now, we estimate $\displaystyle\sum_{i=1}^m \int_{\mathcal{B}_\varepsilon(z_i)} \gamma\{\vartheta_N[f] - \vartheta_N[f](z_i)\}\,\mathrm{d}x$. Using the smoothness of $\vartheta_N[f]$ in $\mathcal{B}_\varepsilon(z_i)$, Taylor's theorem, and the change of variable $x = z_i + \varepsilon y$ for $i = 1, ..., m$, one obtains

$$\vartheta_N[f](z_i + \varepsilon y) = \vartheta_N[f](z_i) + \varepsilon\nabla\vartheta_N[f](\xi_y^i)y,\ \text{ with }\ \xi_y^i \in \mathcal{B}_\varepsilon(z_i).$$

Then there exist a positive constant c independent of ε such that

$$\left|\sum_{i=1}^m \int_{\mathcal{B}_\varepsilon(z_i)} \gamma\{\vartheta_N[f] - \vartheta_N[f](z_i)\}\,\mathrm{d}x\right| = \left|\sum_{i=1}^m \gamma\varepsilon \int_{\mathcal{B}_\varepsilon(z_i)} \nabla\vartheta_N[f](\xi_y^i)(y)\,\mathrm{d}x\right| \le c\ \varepsilon^4 = o(\varepsilon^3). \tag{28}$$

Therefore, from (28) and $|\mathcal{B}_\varepsilon(z_i)| \sim \frac{4\pi}{3}\varepsilon^3$, we have

$$\mathcal{J}_{NN}(f + \delta f_{z,\varepsilon}) - \mathcal{J}_{NN}(f) = \sum_{i=1}^m \varepsilon^3\frac{4\pi}{3}\gamma\vartheta_N[f](z_i) + o(\varepsilon^3). \tag{29}$$

• ***Variation of*** $\mathcal{J}_{DD}$: in a similar way as we get (29), we obtain

$$\mathcal{J}_{DD}(f+\delta f_{z,\varepsilon})-\mathcal{J}_{DD}(f)=\sum_{i=1}^{m}\varepsilon^3\frac{4\pi}{3}\gamma\vartheta_D[f](z_i)+o(\varepsilon^3) \tag{30}$$

with $\vartheta_D[f]\in H_0^1(\Omega)$ is the solution to the adjoint problem:

$$\begin{aligned}\int_\Omega \mathcal{D}\nabla w.\nabla\vartheta_D[f]\,\mathrm{d}x+\int_\Omega \mu w\,\vartheta_D[f]\,\mathrm{d}x\\ =2\int_\Omega \mathcal{D}\nabla\psi_D[f].\nabla w\,\mathrm{d}x,\ \text{for all } w\in H_0^1(\Omega).\end{aligned} \tag{31}$$

• ***Variation of*** $\mathcal{J}_{DN}$: we have

$$\begin{aligned}\mathcal{J}_{DN}(f+\delta f_{z,\varepsilon})-\mathcal{J}_{DN}(f)&=\int_\Omega \mathcal{D}\nabla(\psi_D[f+\delta f_{z,\varepsilon}]-\psi_D[f]).\nabla(\psi_N[f+\delta f_{z,\varepsilon}]-\psi_N[f])\,\mathrm{d}x\\ &+\int_\Omega \mathcal{D}\nabla\psi_N[f+\delta f_{z,\varepsilon}].\nabla\psi_D[f]\,\mathrm{d}x-\int_\Omega \mathcal{D}\nabla\psi_D[f].\nabla\psi_N[f]\,\mathrm{d}x.\\ &+\int_\Omega \mathcal{D}\nabla\psi_D[f+\delta f_{z,\varepsilon}].\nabla\psi_N[f]\,\mathrm{d}x-\int_\Omega \mathcal{D}\nabla\psi_D[f].\nabla\psi_N[f]\,\mathrm{d}x.\end{aligned} \tag{32}$$

Let us first study $\int_\Omega \mathcal{D}\nabla(\psi_D[f+\delta f_{z,\varepsilon}]-\psi_D[f]).\nabla(\psi_N[f+\delta f_{z,\varepsilon}]-\psi_N[f])\,\mathrm{d}x$. Using the Cauchy-Schwarz inequality and Lemma 4.2, we have

$$\begin{aligned}&\left|\int_\Omega \mathcal{D}\nabla(\psi_D[f+\delta f_{z,\varepsilon}]-\psi_D[f]).\nabla(\psi_N[f+\delta f_{z,\varepsilon}]-\psi_N[f])\,\mathrm{d}x\right|\\ &\le c\|\psi_D[f+\delta f_{z,\varepsilon}]-\psi_D[f]\|_{H^1(\Omega)}\|\psi_N[f+\delta f_{z,\varepsilon}]-\psi_N[f]\|_{H^1(\Omega)}\\ &\le c\varepsilon^5.\end{aligned}$$

Then, the first term on the right-hand-side of the equality (32), it can be estimated as

$$\int_\Omega \mathcal{D}\nabla(\psi_D[f+\delta f_{z,\varepsilon}]-\psi_D[f]).\nabla(\psi_N[f+\delta f_{z,\varepsilon}]-\psi_N[f])\,\mathrm{d}x=o(\varepsilon^3). \tag{33}$$

To examine the second terms on the right-hand-side of (32), let us introduce an adjoint stat $\rho_N[f]\in H^1(\Omega)$ as the solution of the following adjoint problem

$$\begin{aligned}\int_\Omega \mathcal{D}\nabla w.\nabla\rho_N[f]\,\mathrm{d}x+\int_\Omega \mu w\,\rho_N[f]\,\mathrm{d}x\\ =\int_\Omega \mathcal{D}\nabla\psi_D[f].\nabla w\,\mathrm{d}x,\ \text{for all } w\in H^1(\Omega).\end{aligned} \tag{34}$$

Then, we have

$$\begin{aligned}&\int_\Omega \mathcal{D}\nabla\psi_N[f+\delta f_{z,\varepsilon}].\nabla\psi_D[f]\,\mathrm{d}x-\int_\Omega \mathcal{D}\nabla\psi_N[f].\nabla\psi_D[f]\,\mathrm{d}x\\ &=\int_\Omega \mathcal{D}\nabla(\psi_N[f+\delta f_{z,\varepsilon}]-\psi_N[f]).\nabla\psi_D[f]\,\mathrm{d}x.\end{aligned}$$

Choosing $w=\psi_N[f+\delta f_{z,\varepsilon}]-\psi_N[f]$ in (34) and $\xi=\rho_N[f]$ in (22) as test functions, we get

$$\int_\Omega \mathcal{D}\nabla(\psi_N[f+\delta f_{z,\varepsilon}]-\psi_N[f]).\nabla\psi_D[f]\,\mathrm{d}x=\int_\Omega \delta f_{z,\varepsilon}\rho_N[f]\mathrm{d}x.$$

Therefore,

$$\int_\Omega \mathcal{D}\nabla\psi_N[f+\delta f_{z,\varepsilon}].\nabla\psi_D[f]\,\mathrm{d}x - \int_\Omega \mathcal{D}\nabla\psi_D[f].\nabla\psi_N[f]\,\mathrm{d}x = \int_\Omega \delta f_{z,\varepsilon}\rho_N[f]\mathrm{d}x$$
$$= \sum_{i=1}^m \gamma|\mathcal{B}_\varepsilon(z_i)|\rho_N[f](z_i)\,\mathrm{d}x + \sum_{i=1}^m \int_{\mathcal{B}_\varepsilon(z_i)} \gamma\{\rho_N[f]-\rho_N[f](z_i)\}\,\mathrm{d}x.$$

Using the same argument as the one used in the deduction of (28), we obtain

$$\Big|\sum_{i=1}^m \int_{\mathcal{B}_\varepsilon(z_i)} \gamma\{\rho_N[f]-\rho_N[f](z_i)\}\,\mathrm{d}x\Big| \le c\varepsilon^4 = o(\varepsilon^3).$$

Consequently,

$$\int_\Omega \mathcal{D}\nabla\psi_N[f+\delta f_{z,\varepsilon}].\nabla\psi_D[f]\,\mathrm{d}x - \int_\Omega \mathcal{D}\nabla\psi_D[f].\nabla\psi_N[f]\,\mathrm{d}x = \sum_{i=1}^m \varepsilon^3\frac{4\pi}{3}\gamma\rho_N[f](z_i) + o(\varepsilon^3). \tag{35}$$

Similarly, we have

$$\int_\Omega \mathcal{D}\nabla\psi_D[f+\delta f_{z,\varepsilon}].\nabla\psi_N[f]\,\mathrm{d}x - \int_\Omega \mathcal{D}\nabla\psi_D[f].\nabla\psi_N[f]\,\mathrm{d}x = \sum_{i=1}^m \varepsilon^3\frac{4\pi}{3}\gamma\rho_D[f](z_i) + o(\varepsilon^3), \tag{36}$$

with $\rho_D[f] \in H_0^1(\Omega)$ is the solution to the following adjoint problem

$$\int_\Omega \mathcal{D}\nabla w.\nabla\rho_D[f]\,\mathrm{d}x + \int_\Omega \mu w\,\rho_D[f]\,\mathrm{d}x$$
$$= \int_\Omega \mathcal{D}\nabla\psi_N[f].\nabla w\,\mathrm{d}x, \text{ for all } w \in H_0^1(\Omega). \tag{37}$$

Gathering (33), (35) and (36), we obtain

$$\mathcal{J}_{DN}(f+\delta f_{z,\varepsilon}) - \mathcal{J}_{DN}(f) = \sum_{i=1}^m \varepsilon^3\frac{4\pi}{3}\gamma\{\rho_D[f](z_i)+\rho_N[f](z_i)\} + o(\varepsilon^3). \tag{38}$$

Combining (29), (30) and (38), the variation of the Kohn-Vogelius functional $\mathcal{J}$ has the form:

$$\mathcal{J}(f+\delta f_{z,\varepsilon}) - \mathcal{J}(f) = \sum_{i=1}^m \varepsilon^3\frac{4\pi}{3}\gamma\{\vartheta_D[f]+\vartheta_D[f](z_i) - 2\rho_D[f] - 2\rho_N[f]\}(z_i) + o(\varepsilon^3).$$

From (25) and (34) one can deduce that the adjoint state $\theta_N[f] \in H^1(\Omega)$ solution to (16) can be written as

$$\theta_N[f] = \vartheta_N[f] - 2\rho_N[f].$$

Similarly, from (31) and (37) the adjoint state $\theta_D \in H_0^1(\Omega)$ solution to (17) can be written as

$$\theta_D[f] = \vartheta_D[f] - 2\rho_D[f].$$

Finally, combining the above equalities the functional $\mathcal{J}$ has the following asymptotic expansion:

$$\mathcal{J}(f+\delta f_{z,\varepsilon}) - \mathcal{J}(f) = \sum_{i=1}^m \varepsilon^3\frac{4\pi}{3}\gamma(\theta_D[f](z_i)+\theta_D[f](z_i)) + o(\varepsilon^3).$$

□

This result was proved in [25] to describe the variation of a Kohn-Vogelius type functional with respect to a single small topological perturbation of sources.

5. Numerical Results

In this section, we present some numerical experiments in three dimensions. The use of the topological gradient aims to give us the number of sources and their qualitative location. We propose a fast and efficient reconstruction procedure. Our numerical algorithm is based on the asymptotic formula (18) to reconstruct and locate an internal bioluminescence source distribution subject to Cauchy data. The measurements data ϕ are synthetic, that is, generated by a numerical computation: we fix a support source ω^*, solve the diffusion problem (3) and extract the measurement ϕ by computing ψ on Γ. To make the numerical simulations presented here, we use $\mathbb{P}_2$ finite elements discretization to solve the problems (16), (17), (9) and (10).

For our numerical results, Ω is the cube $[0,1]^3$. The parameters γ, μ, and μ' are chosen as $\gamma = 1$, the absorption coefficient $\mu = 0.21$ and the reduced scattering coefficient $\mu' = 0.2$. Moreover, having μ and μ', we can derive the diffusion coefficient by relation

$$\mathcal{D} = \frac{1}{3(\mu + \mu')}.$$

In the particular case $f = 0$, the variation of the functional $\mathcal{J}$ with respect to a small topological perturbation $\delta f_{z,\varepsilon} = \chi(z + \varepsilon \mathrm{B}(0,1))$ (i.e $m = 1$), is given by (see Theorem 4.1)

$$\mathcal{J}(\delta f_{z,\varepsilon}) - \mathcal{J}(0) = \varepsilon^3 \delta\mathcal{J}(z) + o(\varepsilon^3), \tag{39}$$

with $\delta\mathcal{J}$ is the topological gradient given by

$$\delta\mathcal{J}(x) = \frac{4\pi}{3}(\theta_N[0] + \theta_D[0])(x), \text{ for all } x \in \Omega, \tag{40}$$

where $\theta_N[0]$ and $\theta_D[0]$ solve respectively problems (16) and (17) with $f = 0$.

Our reconstruction procedure is a non-iterative algorithm based on the following steps.

Non-iterative algorithm:

1. Solve the problems (9) and (10) in Ω with $f = 0$,
2. Solve the problems (16) and (17) in Ω with $f = 0$,
3. Compute the topological gradient function $\delta\mathcal{J}$ defined in (40).
4. Determine the support ω^* of the source term f^*.

The location of ω^* is given by the point $z^* \in \Omega$ where the topological gradient $\delta\mathcal{J}$ is most negative. The size of ω^* is approximated using numerical simulation. Let $\delta_{min} = \delta\mathcal{J}(z^*) \leq \delta\mathcal{J}(x)$ for all $x \in \Omega$, the support source ω^* is approximated as follows

$$\omega^* = \{x \in \Omega, \ \ \delta\mathcal{J}(x) \leq c^* = \alpha^* \delta_{min}\},$$

where $\alpha^* \in (0,1)$ such that

$$\mathcal{J}(\gamma\chi(\omega_{\alpha^*})) \leq \mathcal{J}(\gamma\chi(\omega_\alpha)) \text{ for all } \alpha \in (0,1),$$

with $\omega_\alpha = \{x \in \Omega, \ \ \delta\mathcal{J}(x) \leq c = \alpha\delta_{min}\}$.

Remark 5.1. *In the particular case when the exact support source ω^* is known, the best value α^* of the parameter α can be determined as the minimum of the following error functional,*

$$d_\alpha = [meas(\omega^* \cup \omega_\alpha) - meas(\omega^* \cap \omega_\alpha)]/meas(\omega^*), \ \alpha \in [0,1] \tag{41}$$

where meas(E) is the Lebesgue measure of the set E.

Concerning the mesh, we impose a fixed number of discretization points for the exterior boundary Γ, that is 35 points for each direction (in order to have a uniform mesh $h = 1/35$, see Figure 2).

Next, we show the effectiveness of the proposed reconstruction algorithm by presenting some numerical examples. We will consider four numerical examples. The first one concerns the reconstruction of a ball-shaped source. Then in the second example, we test our algorithm to reconstruct an ellipsoidal-shaped source. While in the third example, we test our numerical algorithm to determine the total number of sources. In the fourth example we investigate the robustness of the numerical algorithm with respect to noisy boundary measurement. All the numerical experiments are done using the free software *FreeFem++*.

5.1. Example 1: Reconstruction of spherical-shaped sources

In this example, we test our algorithm on ball-shaped support source. In Figure 3(a)-(b), we apply the procedure described above on a ball centered at $(0.5, 0.5)$ with radii $r^* = 0.35$ where in Figure 3(a) we plot the sensitivity function $\delta\mathcal{J}$ in Ω (the negative zone of $\delta\mathcal{J}$ is the red zone) while the iso-values of $\delta\mathcal{J}$ are projected on xz-, xy- and yz-planes (i.e $y = 0$, $z = 0$ and $x = 0$ respectively) was presented in Figure 3(b)-(d).

As one can observe in Figure 3(a)-(b), the unknown support of the source is located in the region where the topological gradient $\delta\mathcal{J}$ is the most negative (see Figure 3(a) red zone).

To reconstruct the exact source in Figure 3(a) (ball centered at $(0.5, 0.5)$ with radii $r^* = 0.35$), we minimize the error function d_α and we take $\alpha^* = \arg\min_{\alpha\in(0,1)} d_\alpha$. In order to compute numerically an approximation of the minimum of the function d_α, we divide the interval $(0, 1)$ into M equal subintervals (i.e., of size $1/\mathrm{M}$). We denote by $\alpha_i = i/\mathrm{M}$, $1 \le i \le \mathrm{M}$ the $(\mathrm{M}+1)$ endpoints of these intervals and we take $\alpha^* = \arg\min_{\alpha\in\{\alpha_1,\ldots,\alpha_M\}} d_\alpha$. The reconstruction results are illustrated in Figures 4 and 5.

5.2. Example 2: Reconstruction of ellipsoidal-shaped sources

In this example, the unknown support source ω^* is described by an ellipsoid centered at $(0.5, 0.5, 0.5)$. We represent the detection results in Figure 6. Here again, as one can see from Figure 6, the non-iterative algorithm gives quite efficient reconstruction result of ellipsoid-shaped source.

Next, we prove that the computation of the topological gradient does not depend on the number of sources.

5.3. Example 3: Reconstruction of multiples sources

Now we suppose that the number of sources is unknown and we apply our reconstruction algorithm to find the correct number of balls. More precisely, we reconstruct two balls with centers $z_1^* = (0.5, 0.5, 0.5)$, $z_2^* = (0.8, 0.5, 0.7)$ and with shared radii $r^* = 0.15$. Therefore, from the detection result in Figure 7, we observe that the algorithm reconstruct the location and the number of the sources (two balls) and we give an acceptable approximation of its shape. We emphasize that this result is again obtained in only one iteration. The obtained results serve as a good initial guess for an iterative optimization process based on the shape derivative, for instance, level-set method [3, 27].

5.4. Example 4: Effect of noisy data

Reconstruction stability with respect to the noise level is examined in this example. More precisely, the boundary measurement ϕ is replaced by

$$\phi_\varsigma(x) = \phi(x)(1 + \varsigma \times rand(-1, 1)), \quad x \in \Gamma \tag{42}$$

where $rand(-1, 1)$ is a random number uniformly distributed in $(-1, 1)$ and the scaling parameter $\varsigma > 0$ indicates a relative noise level.

The idea is to verify the stability of the reconstruction algorithm with respect to noisy data. The source configuration is the same as the one when the actual support source ω^* is defined by two balls in example 3 (see Figure 7(a)). The reconstruction results of ω^* with respect to each level of noisy $\varsigma \in \{0.1\%, 0.2\%, 0.5\%, 1.2\%\}$ are presented in Figure 8. One observes that if ς is no more than 5% the algorithm is able to reconstruct the source reasonably and if ς is more than 1.2% the reconstruction becomes completely wrong.

6. Conclusions

In this paper, we consider the inverse source problem for the bioluminescence tomography from measurements on the boundary in three dimensional case. We want to detect the location, the number and the shape of the hidden sources within a body. We transform the detection problem into an optimization problem, where the support of the bioluminescent source distribution is the unknown variable. The Kohn-Vogelius type functional is minimized using the topological sensitivity analysis method. An asymptotic

expansion is derived with the help of preliminary estimation describing the influence of the perturbed source on a Dirichlet and Neumann solutions. The unknown bioluminescent source is reconstructed using a level-set curve of the topological gradient. An accurate and fast reconstruction algorithm is proposed.

The presented approach is general and can be adapted for various geometric inverse source problems.

Acknowledgements

The author would like to thank the professor Maatoug Hassine for his assistance, for many helpful suggestions he made of the manuscript.

References

[1] A. B. Abda, F. B. Hassen, J. Leblond, and M. Mahjoub. Sources recovery from boundary data: a model related to electroencephalography. *Math. Comput. Modelling*, 49(11):2213–2223, 2009.
[2] R. P. Agarwal, E. Karapınar, D. O'Regan, and A. F. Roldán-López-de Hierro. *Fixed point theory in metric type spaces*. Springer, 2015.
[3] S. Amstutz and H. Andrä. A new algorithm for topology optimization using a level-set method. *J. Comput. Phys.*, 216(2):573–588, 2006.
[4] S. Amstutz, S. Giusti, A. Novotny, and E. de Souza Neto. Topological derivative for multi-scale linear elasticity models applied to the synthesis of microstructures. *Internat. J. Numer. Methods Engrg.*, 84(6):733–756, 2010.
[5] S. Amstutz, I. Horchani, and M. Masmoudi. Crack detection by the topological gradient method. *Control Cybernet.*, 34(1):81–101, 2005.
[6] S. Amstutz, A. Novotny, and E. de Souza Neto. Topological derivative-based topology optimization of structures subject to drucker–prager stress constraints. *Comput. Methods Appl. Mech. Engrg.*, 233:123–136, 2012.
[7] M. Andrle, F. B. Belgacem, and A. El Badia. Identification of moving pointwise sources in an advection–dispersion–reaction equation. *Inverse Problems*, 27(2):025007, 2011.
[8] M. Andrle and A. El Badia. Identification of multiple moving pollution sources in surface waters or atmospheric media with boundary observations. *Inverse problems*, 28(7):075009, 2012.
[9] Y. E. Anikonov, B. Bubnov, and G. Erokhin. *Inverse and ill-posed sources problems*, volume 9. Walter de Gruyter, 1997.
[10] H. Brezis. *Functional analysis, Sobolev spaces and partial differential equations*. Springer Science & Business Media, 2010.
[11] H. S. Cabayan and G. G. Belford. On computing a stable least squares solution to the inverse problem for a planar newtonian potential. *SIAM J. Appl. Math.*, 20(1):51–61, 1971.
[12] A. Canelas, A. Laurain, and A. A. Novotny. A new reconstruction method for the inverse source problem from partial boundary measurements. *Inverse Problems*, 31(7):075009, 2015.
[13] X. Cheng, R. Gong, and W. Han. A new general mathematical framework for bioluminescence tomography. *Comput. Methods Appl. Mech. Engrg.*, 197(6):524–535, 2008.
[14] L. Ćirić. Some recent results in metrical fixed point theory. 2003.
[15] L. Ćirić, A. Rafiq, S. Radenović, M. Rajović, and J. S. Ume. On mann implicit iterations for strongly accretive and strongly pseudo-contractive mappings. *Appl. Math. Comput.*, 198(1):128–137, 2008.
[16] L. Ćirić, A. Razani, S. Radenović, and J. S. Ume. Common fixed point theorems for families of weakly compatible maps. *Comput. Math. Appl.*, 55(11):2533–2543, 2008.
[17] D. Dukic, L. Paunovic, and S. Radenovic. Convergence of iterates with errors of uniformly quasi-lipschitzian mappings in cone metric spaces. *Kragujevac J. Math.*, 35(3):399–410, 2011.
[18] A. El Badia and T. Nara. An inverse source problem for helmholtz's equation from the cauchy data with a single wave number. *Inverse Problems*, 27(10):105001, 2011.
[19] S. Garreau, P. Guillaume, and M. Masmoudi. The topological asymptotic for pde systems: the elasticity case. *SIAM J. Control Optim.*, 39(6):1756–1778, 2001.
[20] A. Hamdi. Detection-identification of multiple unknown time-dependent point sources in a 2 d transport equation: application to accidental pollution. *Inverse Probl. Sci. Eng.*, 25(10):1423–1447, 2017.
[21] W. Han, W. Cong, and G. Wang. Mathematical theory and numerical analysis of bioluminescence tomography. *Inverse Problems*, 22(5):1659, 2006.
[22] W. Han, K. Kazmi, W. Cong, and G. Wang. Bioluminescence tomography with optimized optical parameters. *Inverse Problems*, 23(3):1215, 2007.
[23] M. Hanke and W. Rundell. On rational approximation methods for inverse source problems. *Inverse Probl. Imaging*, 5(1):185–202, 2011.
[24] M. Hintermüller and A. Laurain. Multiphase image segmentation and modulation recovery based on shape and topological sensitivity. *J. Math. Imaging Vision*, 35(1):1–22, 2009.
[25] M. Hrizi and M. Hassine. One-iteration reconstruction algorithm for geometric inverse source problem. *J. Elliptic Parabol. Equ.*, 4(1):177–205, 2018.
[26] M. Hrizi, M. Hassine, and R. Malek. A new reconstruction method for a parabolic inverse source problem. *Appl. Anal.*, pages 1–33, 2018.
[27] V. Isakov, S. Leung, and J. Qian. A fast local level set method for inverse gravimetry. *Commun. Comput. Phys.*, 10(4):1044–1070, 2011.

[28] K. Ito and J.-C. Liu. Recovery of inclusions in 2d and 3d domains for poisson's equation. *Inverse Problems*, 29(7):075005, 2013.
[29] L. Jaafar-Belaid, M. Jaoua, M. Masmoudi, and M. Siala. Image restoration and edge detection by topological asymptotic expansion. *Tendances des Applications Mathématiques*, page 47, 2006.
[30] M. Jleli, B. Samet, and G. Vial. Topological sensitivity analysis for the modified helmholtz equation under an impedance condition on the boundary of a hole. *J. Math. Pures Appl.*, 103(2):557–574, 2015.
[31] R. V. Kohn and M. Vogelius. Relaxation of a variational method for impedance computed tomography. *Comm. Pure Appl. Math.*, 40(6):745–777, 1987.
[32] T. Kreutzmann and A. Rieder. Geometric reconstruction in bioluminescence tomography. *Inverse Probl. Imaging*, 8:173–97, 2014.
[33] J.-C. Liu. An inverse source problem of the poisson equation with cauchy data. *Electron. J. Differential Equations*, 2017(119):1–19, 2017.
[34] C. G. Lopes, R. B. dos Santos, A. A. Novotny, and J. Sokołowski. Asymptotic analysis of variational inequalities with applications to optimum design in elasticity. *Asymptot. Anal.*, 102(3-4):227–242, 2017.
[35] C. G. Lopes and A. A. Novotny. Topology design of compliant mechanisms with stress constraints based on the topological derivative concept. *Struct. Multidiscip. Optim.*, 54(4):737–746, 2016.
[36] A. A. Novotny and J. Sokołowski. *Topological derivatives in shape optimization*. Springer Science & Business Media, 2012.
[37] B. Samet, S. Amstutz, and M. Masmoudi. The topological asymptotic for the helmholtz equation. *SIAM J. Control Optim.*, 42(5):1523–1544, 2003.
[38] J. Sokołowski and A. Żochowski. Topological derivative for optimal control problems. *Control Cybernet.*, 28:611–625, 1999.
[39] V. Todorčević. *Harmonic quasiconformal mappings and hyperbolic type metrics*. Springer, 2019.
[40] V. Todorčević. Subharmonic behavior and quasiconformal mappings. *Anal. Math. Phys.*, 9(3):1211–1225, 2019.
[41] N. Van Goethem and A. Novotny. Crack nucleation sensitivity analysis. *Math. Methods Appl. Sci.*, 33(16):1978–1994, 2010.
[42] G. Wang, Y. Li, and M. Jiang. Uniqueness theorems in bioluminescence tomography. *Medical physics*, 31(8):2289–2299, 2004.

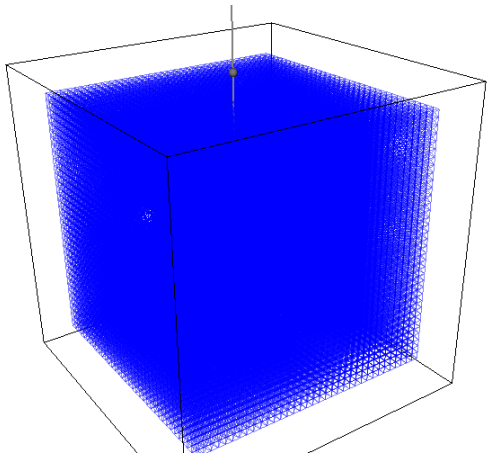

Figure 2: Discretization of the domain Omega.

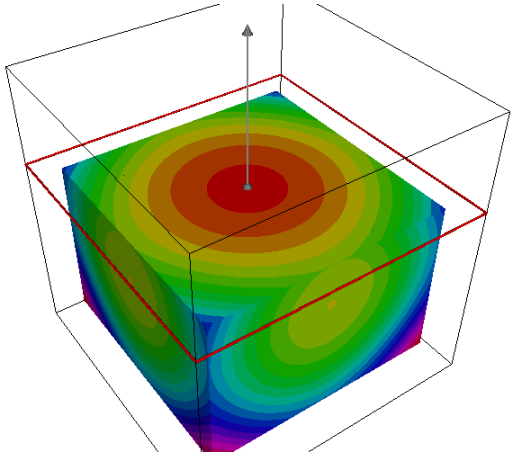

(a)Topological gradient $\delta\mathcal{J}$ in Ω

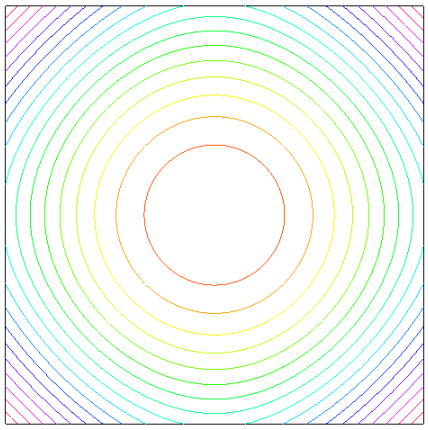

(b)Isovalues of $\delta\mathcal{J}$ projected on xz-plane

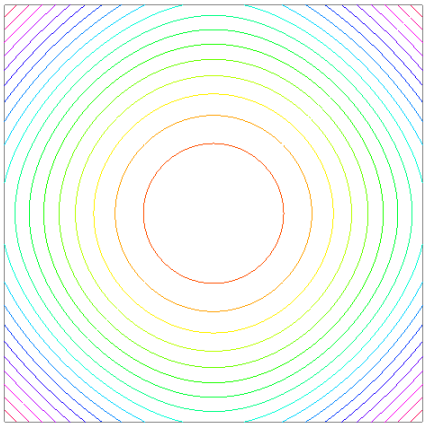

(c) Isovalues of $\delta\mathcal{J}$ projected on xy-plane

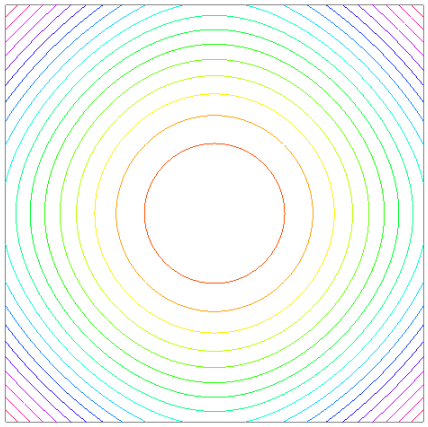

(d) Isovalues of $\delta\mathcal{J}$ projected on yz-plane

Figure 3: Topological gradient and the isovalues projected on xz-, xy- and yz-planes

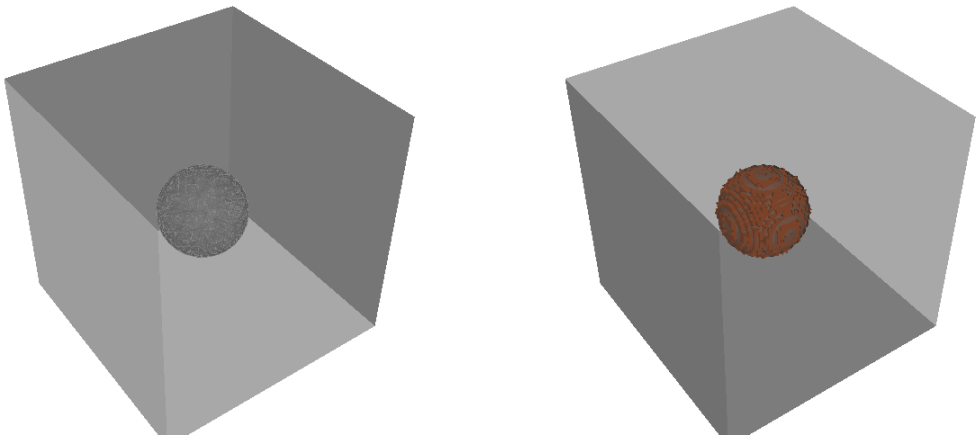

(a) True source term (b) Reconstruction with $\alpha^* = 0.42$

Figure 4: Reconstruction of ball-shaped source

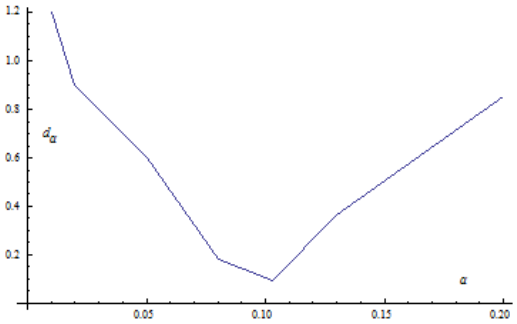

Figure 5: The variation of the error function d_α with respect to α

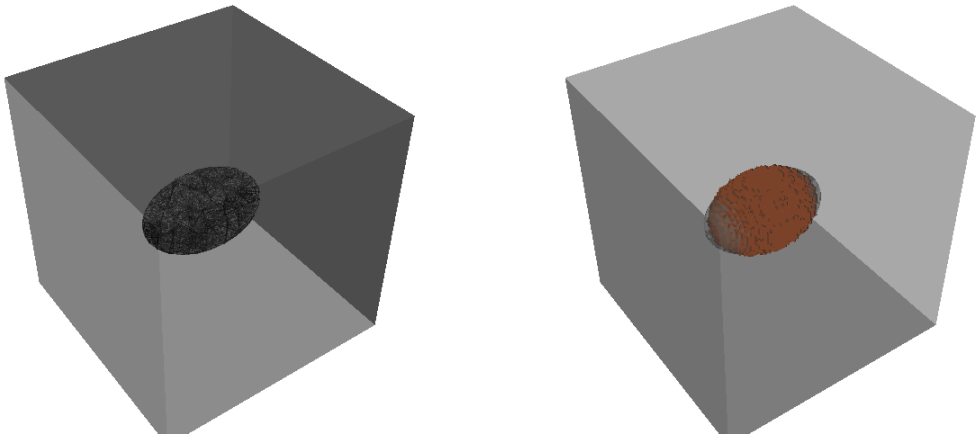

(a) True source term (b) Reconstruction $\alpha^* = 0.75$

Figure 6: Reconstruction of ellipsoidal-shaped source

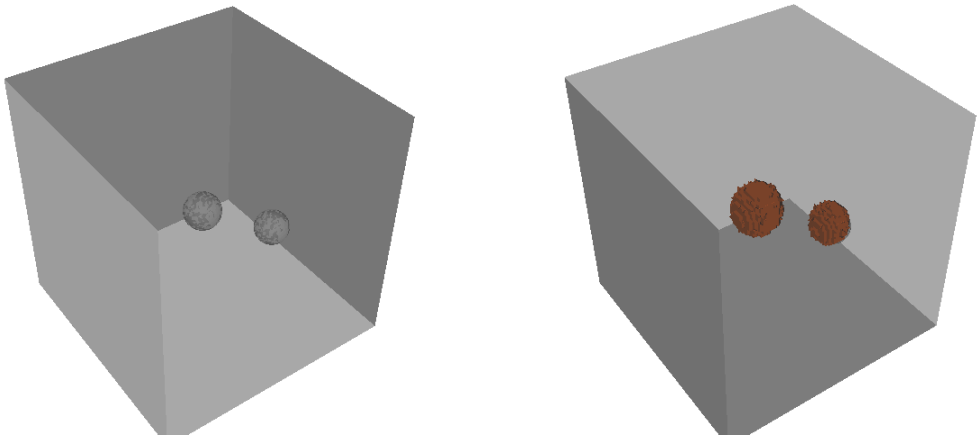

(a) True source term (b) Reconstruction $\alpha^* = 0.016$

Figure 7: Reconstruction of two balls

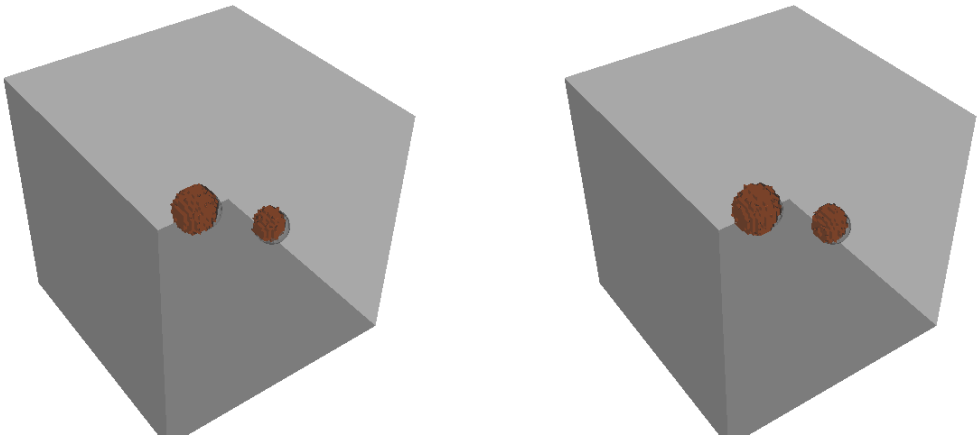

(a) $\alpha^* = 0.016$ and $\varsigma = 0.1\%$ (b) $\alpha^* = 0.016$ and $\varsigma = 0.2\%$

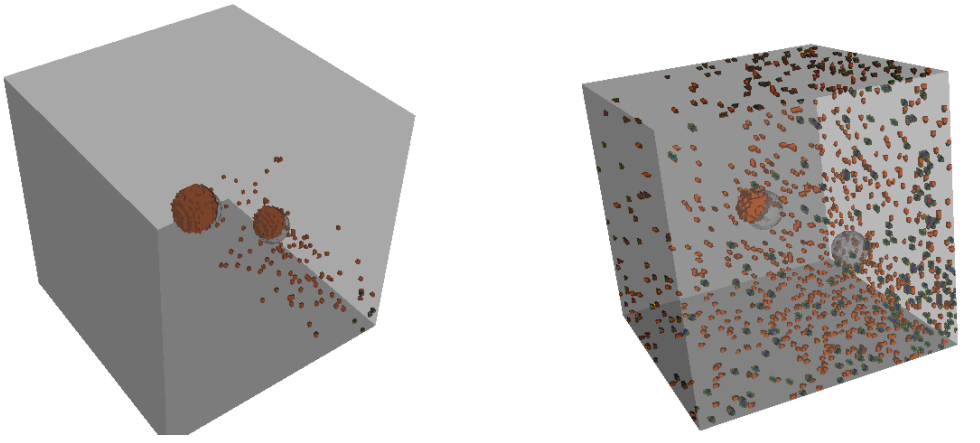

(c) $\alpha^* = 0.016$ and $\varsigma = 0.5\%$ (d) $\alpha^* = 0.016$ and $\varsigma = 1.2\%$

Figure 8: Effect of noisy data